MITSUBISHI ELECTRIC RESEARCH LABORATORIES
http://www.merl.com

Modeling and Control of Radiant, Convective, and Ventilation Systems for Multizone Residences

Laughman, C.R.; Mackey, C.; Bortoff, S.A.; Qiao, H.

TR2019-093 September 05, 2019

Abstract

The variety of ventilation requirements, thermal comfort specifications, and lower cooling loads for highperformance buildings can motivate the use of multiple HVAC systems whose dynamic interactions can strongly affect performance. We develop a Modelica energy model of a multi-zone residential building, based on an prototype EnergyPlus model distributed by the U.S. DOE, to quantify these interactions and design new controls to improve comfort. Fully dynamic radiant, convective, and ventilation subsystems are all integrated into a heterogeneous cooling system that has better performance than is achievable by a smaller collection of systems.

Building Simulation

Modeling and Control of Radiant, Convective, and Ventilation Systems for Multizone Residences

Christopher R. Laughman[1], Chris Mackey[2], Scott A. Bortoff[1], Hongtao Qiao[1]
[1]Mitsubishi Electric Research Laboratories, Cambridge, MA, USA
[2]Ladybug Tools, Fairfax, VA, USA

Abstract

The variety of ventilation requirements, thermal comfort specifications, and lower cooling loads for high-performance buildings can motivate the use of multiple HVAC systems whose dynamic interactions can strongly affect performance. We develop a Modelica energy model of a multi-zone residential building, based on an prototype EnergyPlus model distributed by the U.S. DOE, to quantify these interactions and design new controls to improve comfort. Fully dynamic radiant, convective, and ventilation subsystems are all integrated into a heterogeneous cooling system that has better performance than is achievable by a smaller collection of systems.

Introduction

High-performance buildings often share a few common characteristics, such as significantly reduced infiltration and superinsulated envelopes that drastically reduce the space loads with potentially large reductions in the sensible heat factor. The substantial increase in measured energy efficiency for these buildings, as well as the improvements to thermal comfort attainable in these spaces, has a prompted a surge in the construction of these types of buildings. These characteristics can present a host of challenges for HVAC systems, however, motivating research and exploration of a variety of new configurations of ventilation, convective, and radiant space conditioning systems to improve thermal comfort and occupant health.

One of the challenges faced when designing HVAC systems for high-performance residential buildings is that the reduced size of the mechanical systems and the wide variety of installed systems are accompanied by dynamic interactions between components of the overall system. Unlike conventional systems, which often have high heating or cooling capacities and operate at low part-load efficiencies, the mechanical equipment for high-performance buildings have much lower capacities and are not designed to reject large temperature or heat load disturbances. As a result, the hygrothermal building dynamics can be much more sensitive to the equipment operation and the coupled behavior resulting from subsystem interactions than conventional buildings.

Unfortunately, such interactions are rarely described by the equipment models used in most common building energy simulation environments, which often eliminate these dynamics to simplify their models or simulations. As an example, models of variable refrigerant flow systems used in EnergyPlus (Hong et al., 2016) have no dynamics, but only use algebraic relations to describe the input/output characteristics of the systems. Such simplifications will therefore be blind to both the opportunities for improvement in system performance that might be attained by effective operation and coordination between systems, as well as to limit cycles or inefficient operation that can be accompanied by poorly designed controls. While these problems are notoriously difficult and expensive to solve after construction, they can be effectively addressed at a much earlier stage via dynamic simulation and systematic controls design.

While many alternative system architectures for high-performance buildings have been studied, there has been somewhat less attention dedicated to the dynamics associated with couplings between the building envelope and multiple mechanical systems. Seminal work on the combined use of dedicated outdoor air systems (DOAS) and radiant systems to achieve energy savings was done by Jeong et al. (2003). Similarly, Gayeski et al. (2011) used a series of temperature- and load-dependent maps for a variable capacity chiller to perform predictive precooling of a concrete-core radiant floor coupled to an air-source heat pump, and experimentally demonstrated energy savings of 19-25% in Atlanta and Phoenix climate conditions for this innovative system. The present paper extends recent work by the authors presented in Laughman et al. (2018), in which we explored the operation of a multi-zone air-source heat pump with multiple ventilation systems in cooling mode.

Modelica (Modelica Association, 2017) is emerging in the building science community as a powerful tool for studying the dynamics of these complex multiphysical systems. The equation-oriented design of the language enables the creation of physics-based component models that can be interconnected to form large dynamical systems, such as vapor compression cycles or buildings. This equation-based representation also enables uses of these models beyond simulation, such as control design or optimization. The open-source nature of the language has also facilitated the creation of high quality publicly-available model libraries, such as the Buildings Library (Wetter et al., 2014), which is used extensively in this work.

The objective of this paper is the study and management of the coupled behavior of convective, radiant, and ventilation mechnical subsystems in a 2-zone residential building under cooling conditions. Because the success of this investigation depends strongly upon the accuracy of the building energy model, we also demonstrate a process by which building energy models generated in EnergyPlus (Crawley et al., 2000), a widely used building energy modeling tool, can be mapped into equivalent Modelica models. We then use these models to analyze and design coordinated controls for the coupled dynamics of these three subsystems; while convective and radiant systems are not often used for the same space, their coordinated operation enables the management of thermal comfort over much shorter timescales than is otherwise possible.

The structure of this paper is as follows. In the following section, we briefly describe the EnergyPlus residential building energy model used in this work and outline the translation process used to generate the Modelica model, the accuracy of which is indicated by a comparison of two representative simulation outputs. We then provide an overview of the dynamic physics-based equipment models for the multi-zone air-source heat pump (variable refrigerant flow system, or VRF) and the DOAS, and describe some nonintuitive dynamics of the system to demonstrate the effect of dynamics on the overall building operation. With the results of this analysis, we design a coordinated controller that manages the operation of all three mechanical systems and demonstrate its effectiveness on the overall system model. Finally, we briefly outline a set of conclusions and describe future work in this area.

Building Models

The study of the coupled behavior of the individual HVAC subsystems is strongly dependent upon the building energy model, as the dynamics of the cooling load are shaped by the building envelope. We thus identified a set of residential prototype building energy models in EnergyPlus that were created by the U.S. Department of Energy in 2015 that represent typical building construction in each of the 50 states (Taylor et al., 2015). This model corresponding to Georgia was then adapted for this work so that we could investigate the building dynamics for a mixed-humid climate zone. The EnergyPlus models were particularly attractive as a starting point because of our interest in exploring and validating a process of converting the common structure of EnergyPlus models to those of Modelica. While Modelica building models have been validated in the context of ASHRAE Standard 140 for a room model (Nouidui et al., 2012), there is little literature describing this process in practice.

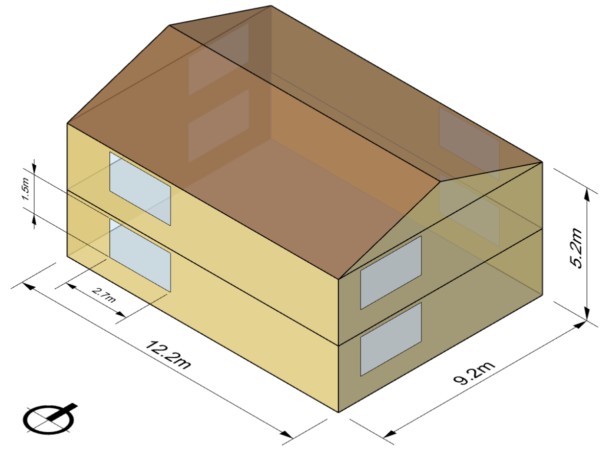

Figure 1: Illustration of prototype residence.

The building model, illustrated in Figure 1, consists of a two-story residence with nominal 2009 IECC-based construction. Each floor of this residence has a floor area of 112.24 m^2 and is 2.6 m tall, and is oriented along the cardinal directions with a peak occupancy of 3 people per floor. Each exterior wall also has a window that was 1.52 m by 2.72 m that admits solar heat gains into the spaces. A few modifications to this model were necessary because of differences in modeling assumptions between EnergyPlus and Modelica; while the original model only used a single zone for the entire residence, we separated the upper floor and lower floor into separate zones to allow us to study the differing dynamics of both spaces. We also added a 10 cm thick concrete slab and 2 meters of soil below the house to characterize the thermal boundary condition under the house with a boundary of 21 °C, and simplified the window models to be single panes for simplicity. A cross-sectional schematic illustrating the house with its associated radiant, convective, and ventilation systems is illustrated in Figure 2.

The Modelica Buildings library uses physics-based models to describe the dynamic behavior of buildings and their systems. Many of these models are 1-D models; wall constructions typically only have temperature variation through their cross-section. The air volumes use a mixed-air assumption with simplified moist-air media, while the star network approximation is used to describe the radiant heat transfer (Wetter et al., 2014). The architecture of this library is well-suited to the adaptation of EnergyPlus models because the geometric and material data for both simulation enviroments can be specified by using a series of hierarchical objects. In general, the

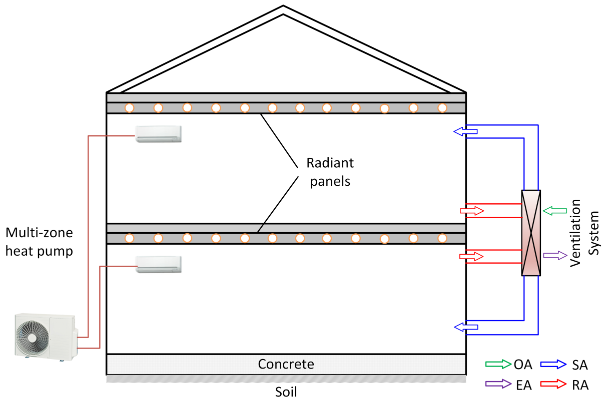

Figure 2: Overall system schematic.

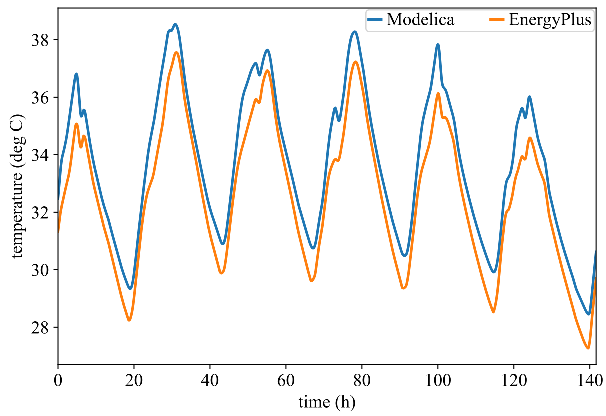

Figure 3: Comparison of ground floor convective zone temperature outputs from EnergyPlus and Modelica.

`.idf` files used to capture the simulation information in EnergyPlus can be divided into a number of classes of data structures, corresponding to surface constructions (e.g., walls), construction details (e.g., specific wall cross-sections), material properties, and heat gain schedules. As an example, the exterior wall construction in the building is encoded in EnergyPlus as follows (with some minor simplifications for brevity):

```
Construction,
 Exterior Wall,            !- Name
 Stucco_1in,               !- Layer 1
 sheathing_consol_layer,   !- Layer 2
 OSB_5/8in,                !- Layer 3
 wall_consol_layer,        !- Layer 4
 Drywall_1/2in;            !- Layer 5
```

The Buildings library models are structured similarly to the EnergyPlus models to take advantages of the intuitive divisions between materials, constructions, and rooms, allowing the user to define material objects and then assemble multiple constructions without the use of repetitive definitions. One important difference is that the Buildings library assumes cuboid geometries for the rooms to simplify the model representation. In analogy to the EnergyPlus construction model for `Exterior Wall`, the construction record in the Buildings library is represented as

```
record ExteriorWall
 import BL=
  Buildings.HeatTransfer.Data.OpaqueConst
 import MEB=MEBuildings.Records.Materials
 extends BL.Generic(
  material=MEB.Stucco_OneIn(x=0.0254),
           MEB.Sheathing_consol_layer(x=0.013),
           MEB.OSB_FiveEighthIn(x=0.0159),
           MEB.Wall_consol_layer(x=0.140),
           MEB.Drywall_OneHalfIn(x=0.0127),
  final nLay=5);
end ExteriorWall;
```

The mapping of surface constructions and materials is analogous for many standard building geometries, and is thus relatively straightforward.

One of the main advantages of the equation-oriented structure of Modelica is that the system composition can be changed quite dramatically. The overall building model was thus assembled to allow the construction between the floors to be replaced, which enabled the standard floor used in the base energy model to be replaced with an assembly consisting of a radiant panel and a standard floor. This radiant floor was adapted from the `Buildings.Fluid.HeatExchangers.RadiantSlab` model, in which the hydronic pipes are embedded in a building construction. In this case, the panel consists of a sheet of 4.75 mm thick aluminum sheet with 17 mm PEX pipes spaced 15 cm apart, backed by 5 cm thick expanded foam insulation and standard wood construction.

While this radiant panel/floor model was used to study the system dynamics and controls later in this work, it was first necessary to validate the performance of the Modelica model against the output of the EnergyPlus model. These models were thus both simulated for 1 year using the Atlanta-Hartsfield TMY3 file to perform this comparison. We imposed no internal load on the space in these simulations because our primary interest was in comparing the hygrothermal dynamics of the envelope. Since the dynamics of the HVAC systems necessarily differ between EnergyPlus and Modelica, the inclusion of such systems would make it difficult to compare the performance of the envelopes. While most parameters of these simulations were set to identical values for this comparison, but we found that adjusting the SHGC was important to achieve a reasonable match between the simulations. Since only a single-pane glass window construction was used in Modelica, we set the SHGC for the windows in EnergyPlus to 0.65.

Table 1 and Figure 3 illustrate the good agreement

Floor	Variable	RMSE/year
Ground	$\mathrm{T_{room}}$	1.11 °C
Upper	$\mathrm{T_{room}}$	0.836 °C
Ground	$\mathrm{T_{rad}}$	1.11 °C
Upper	$\mathrm{T_{rad}}$	0.987 °C
Ground	ϕ_{room}	2.75%
Upper	ϕ_{room}	2.31%

Table 1: Residual errors between annual simulations in EnergyPlus and Modelica for both zones.

between the two building energy simulations. The temperature data over 6 days for the ground floor zone illustrates the similarity of the dynamics between the two simulation outputs, which is perhaps of highest importance when studying the dynamic behavior of the conditioned building. It is also encouraging to see good agreement between the simulations via the root mean squred error (RMSE); while these two models do not make exactly the same assumptions, the Modelica model is sufficiently close to the EnergyPlus model with RMSEs on the order of 1 °C or 2% RH that it can be profitably used to study the dynamics of a building with radiant, convective, and ventilation.

Equipment Models

Dynamic physics-based models of both a VRF system and a DOAS were used to explore the interactions of radiant, convective, and ventilation systems in this work. Because these cycles are both assembled from similar components, we will briefly describe the component models (e.g., multiphase heat exchangers, compressors, expansion valves) and then describe how these component models are used to build the complete cycle models.

One common set of experimentally-validated assumptions is that the dynamics of the heat exchangers (HEXs) dominate the temporal behavior of vapor-compression cycles over most timescales of interest. As such, the component models used employ dynamic models of the HEXs and static (algebraic) models of the compressors, expansion valves, and fans. We used finite volume models (Qiao et al., 2015) to describe the dynamic behavior of the HEXs to capture the behavior of the refrigerant pressures, which can vary significantly due to line lengths and affect important control variables like the suction superheat temperature, and also to capture the spatially-varying behavior of the models. Other common modeling assumptions, described in Qiao et al. (2015), were used to ensure that the models had suitable performance.

Under these assumptions, the Navier-Stokes equations describing the conservation of mass, momentum, and energy can be discretized to describe 1-D multiphase refrigerant flowfor these finite volume models by using an upwind difference method for this

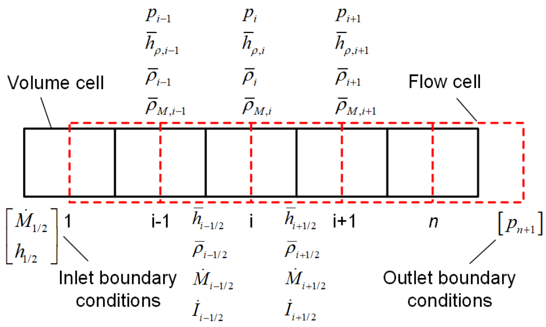

Figure 4: Finite volume discretization of refrigerant pipe.

convection-dominated flow. Figure 4 illustrates the staggered grid scheme that is used to avoid nonphysical numerical phenomena by decoupling the mass and energy equations computed for the volume cells (black solid boundary) from the momentum equations computed for the flow cells (red dashed boundary), resulting in the equations

$$A_c \Delta z \rho_i = \dot{M}_{i-1/2} - \dot{M}_{i+1/2}, \tag{1}$$

$$\Delta z \frac{\mathrm{d}\dot{M}_{i+1/2}}{\mathrm{d}t} = \dot{I}_i - \dot{I}_{i+1} - A_c(p_{i+1} - p_i) - P\Delta z \bar{\tau}_{w,i+1/2}, \tag{2}$$

$$A_c \Delta z u_i = \dot{M}_{i-1/2}(h_{i-1/2} - \bar{h}_{\rho,i}) - \dot{M}_{i+1/2}(h_{i+1/2} - \bar{h}_{\rho,i}) + P\Delta z q_i'', \tag{3}$$

where $\bar{\rho}_M$ represents the momentum density, $\bar{h}_\rho$ and $\bar{h}$ signify the the density-weighted and flow-weighted specific enthalpies, the wall shear stress $\bar{\tau} = \frac{1}{2} f \bar{\rho} u \,|u|$ and f is the Fanning friction factor, P is the circumference of the flow channel, and symbols with overbars represent average quantities in each cell. The dynamic states used in this model include the refrigerant pressures p and the density-weighted specific enthalpies $\bar{h}_\rho$.

A set of simplified closure relations for the frictional pressure drop and the refrigerant-side heat transfer coefficients were used because many correlations from the literature have poor numerical properties that make them unsuitable for inclusion in a dynamic simulation. The frictional pressure drop was expressed as $\Delta p/\dot{M}^2 = K\left(\Delta p_0/\dot{M}_0^2\right)$, while simplified heat transfer relations (HTC) were also used in which each phase HTC was only dependent upon the refrigerant mass flow rate, and the smooth transition between the phases was enforced via trigonometric interpolation. We also introduced fast dynamics in the HTC to eliminate algebraic couplings between the pipe wall states and the refrigerant property states, as described by Laughman and Qiao (2018), and thereby eliminated non-physical high-frequency behavior and described the low-pass effect of refrigerant oil.

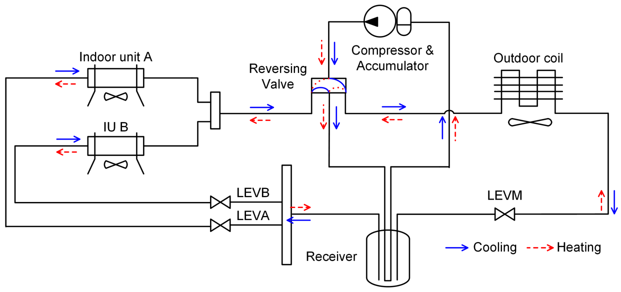

Figure 5: Construction of VRF system.

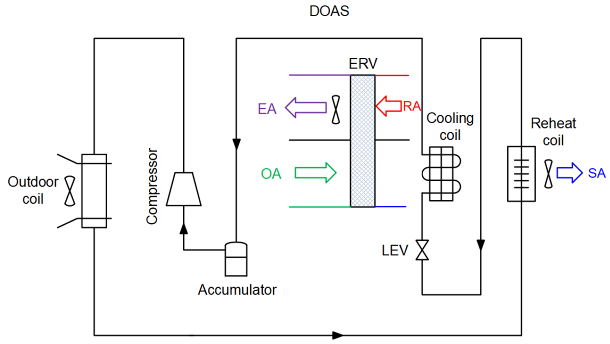

Figure 6: Construction of DOAS with reheat coil.

Standard one-dimensional models of the heat conduction through the refrigerant wall were used, as well as the heat convection to the moist air; these are described in detail by Qiao et al. (2015). One aspect of these models that was important for simulation was the use of a gas law in which the pressure and temperature are assumed to be independent, so that

$$\rho/\rho_{stp} = p/p_{stp} \tag{4}$$

where ρ_{stp} and p_{stp} are the density and pressure at a constant reference (Wetter et al., 2014). This allows for smaller systems of nonlinear equations, which became significant in this model because of the degree to which the different equipment models were coupled through the air model.

A simple isenthalpic model of the electronic expansion valve was also used, as described by a standard orifice flow equation

$$\dot{M} = C_v a_v \sqrt{\rho_{in} \Delta P}, \tag{5}$$

where the flow coefficient C_v and was determined experimentally, the orifice flow area a_v was modulated to control the cycle behavior, and the mass flow rate is regularized in the neighborhood of zero flow.

A one dimensional model of the variable-speed rotary compressor was used in which the performance was described by relating the volumetric efficiency η_v and isentropic efficiency η_{is} to the suction pressure P_{suc}, discharge pressure P_{dis}, and compressor frequency f, as given by

$$\eta_v = \frac{\dot{M}_{comp}}{\rho_{suc} V f} \tag{6}$$

$$\eta_{is} = \frac{h_{dis,isen} - h_{suc}}{h_{dis} - h_{suc}}. \tag{7}$$

The oefficients used for the functional forms of η_v, η_{is}, and the compressor power consumption $\dot{W}$ were derived from experimental data. Algebraic models were also used for the fans and energy recovery wheel to capture the salient behavior. More information on this menagerie of component models needed to construct the full equipment models is available in Laughman et al. (2018).

These component models were used to assemble a VRF system model with a separate evaporator located in each indoor space, as illustrated in Figure 5 and briefly described here. The hot discharge gas leaving the compressor first condenses to a liquid as it travels through an outdoor heat exchanger, and then is partially expanded as it passes through a first valve (LEVM) and into a high-side receiver. Upon leaving the receiver, it splits into a manifold that connects to the indoor units. The refrigerant in each branch then passes through a second smaller expansion valve which is designed to regulate the amount of cooling in each zone by metering the refrigerant, and flows through adiabatic refrigerant pipes that are between 11 and 13 meters long. This refrigerant evaporates as it passes through each heat exchanger, providing both sensible and latent cooling to the space, after which returns to the compressor via a second manifold. Standard tube-fin heat exchangers were used to construct this cycle, which is described in more detail in Qiao et al. (2017).

The dynamics of the DOAS system differ from those of the VRF system because of the presence of the reheat coil, as shown in Figure 6. This system effectively splits the refrigerant condensing area between the outdoor HEX and the reheat HEX, so that the some of the heat rejected by the compressor is used to efficiently reheat the air entering the occupied space. Once the refrigerant condenses in the reheat coil, it is expanded and passes through the cooling coil to the suction port of the compressor. The presence of this reheat coil can be very important for DOAS systems because deep dehumidification with standard vapor compression cycles will often overcool the discharge air down to under 10 °C to achieve the desired humidity ratio. By using the reheat coil, the ventilation air delivered to the space can be maintained much closer to the room temperature while simultaneously removing the moisture introduced by the ambient air.

The importance of understanding and managing the coupled system dynamics can be seen by considering a scenario with a moderate room temperature of 24.2 °C and a relatively high relative humidity (75%) for the ground floor zone in which the compressor frequency of the VRF system is increased by 10 Hz at a point in time, as illustrated in Figure 7. While the intuitive expectation for this scenario would be that

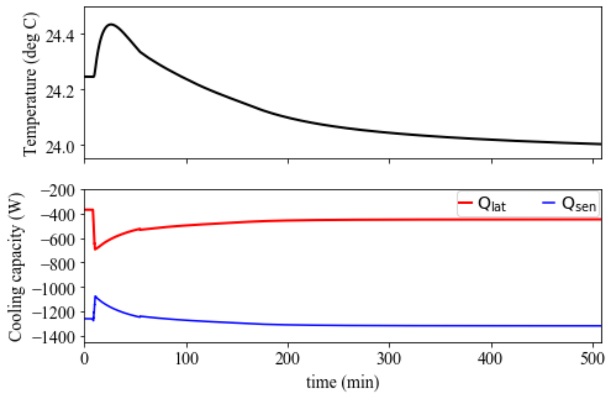

Figure 7: Ground floor zone temperature transient after 10 Hz step in compressor speed.

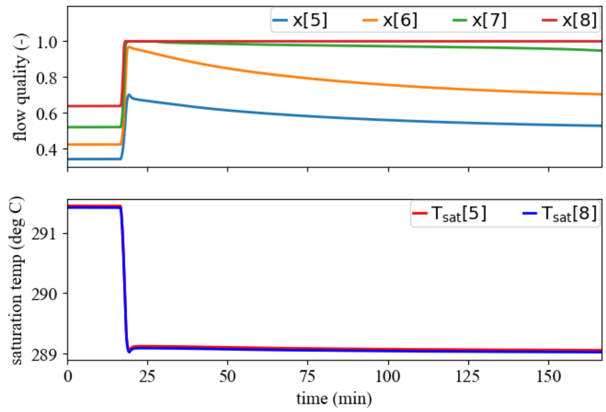

Figure 8: Flow qualities and saturation temperatures for volumes in ground floor zone heat exchanger for VRF system during compressor step transient.

the room temperature for this zone, seen in the upper figure, would immediately start to decrease after the increase in compressor speed, the room temperature actually increased for a period of time before eventually decreasing. This phenomena, known as a non-minimum phase response, has significant ramifications for the design of the control system that will be described in the following section.

The source of this response can be understood by separately considering the latent and sensible coil capacities shown in the lower plot of Figure 7. Immediately after the change in the compressor frequency, we can see that the magnitude of the latent cooling capacity increases, but that the magnitude of the sensible cooling capacity decreases; this drop in the sensible capacity causes the temporary rise in room temperature.

The cause of these different capacity dynamics can be further understood by considering the plots of the flow quality x and the saturation temperature T_{sat}, shown in Figure 8 for a number of distinct volumes in the corresponding indoor heat exchanger; the index number of these volumes increase from the refrigerant pipe inlet to the outlet. The bottom plot of this figure shows that the saturation temperature in all of the volumes decreases, as would be expected with the increase in the compressor speed. This saturation temperature is the refrigerant temperature over the portion of the HEX that has evaporating flow, implying that the 2-phase portion of the coil will quickly get colder.

The upper portion of this figure, illustrating the flow qualities that indicate the liquid/vapor fraction of refrigerant in the 2-phase region, tells a somewhat complimentary story, however. The rapid increase in the refrigerant qualities after the increase in compressor speed suggests that part of the HEX begins to dry out, so that the effective sensible heat capacity of the two-phase region is momentarily reduced, before gradually recovering. This can be further understood by approximating the capacity of the coil as dominated by the two-phase region, so that $Q_{sen} = UA_{2\phi}\Delta T$; while ΔT increases almost immediately, we see that the area of the two-phase region $A_{2\phi}$ decreases because volumes 7 and 8 dry out, resulting in this non-minimum phase behavior. Over time, the recovery of volumes 5 and 6 bring the size of the two-phase region closer to its previous state, and the total sensible capacity increases because of the larger temperature difference. These dual observations explain the transient behavior of the two coil capacities: the latent capacity increases in magnitude because the coil gets colder and the system is better able to dehumidify the air, but the magnitude of the sensible capacity temporarily decreases because the length of the two-phase region shrinks.

System Controls

In this section we present a model-based design for coordinated control of the integrated HVAC system. Our performance requirements are as follows:

1. Track constant zone temperature set-points with zero steady-state error, if possible.
2. Track constant ceiling temperature set-points with zero steady-state error, if possible.
3. Track a constant indoor humidity set-point with zero steady-state error, if possible.
4. Maintain a positive superheat set-point in all evaporators.
5. Enforce constraints on all actuators.
6. Allow for separate operation of each piece of equipment.

Our design results in a separate controller for each piece of equipment. However, each controller must be designed taking into account the dynamic interactions with the other two systems and the building. Requirements 1 and 2 are for human comfort, which is equally a function of both the air temperature and mean radiant temperature in office building conditions. Requirement 4 ensures the system operates efficiently, but is also necessary to counter-act the non-minimum phase response of the VRF system that was discussed earlier. Each of the actuators has hard limits to its range of operation, and the control system must be designed to be robust to these constraints. Of course, it must be possible to operate the VRF, radiant system, and DOAS separately, i.e., turn any of them on or off.

We numerically linearize the 919-dimensional Modelica model, and though a sequence of modal decompositions, Hankel norm truncations and singular perturbations, we compute a more manageable reduced-order model with 30 states that inherits the critical characteristics of the full-order model. An important feature of Modelica compilers is that a linearization can be computed, enabling model-based control design. However, the model libraries e.g., Wetter et al. (2014) contain redundant states, such as alternative state variable representations for fluids, and these result in unobservable modes with zero eigenvalues in the full-order linearization. These are removed symbolically prior to the numerical Hankel-norm truncation. The frequency response of the resulting reduced-order model is then used to design the control system configuration and tune values for its compensators using conventional multivariable loop-shaping methods described in Skogestad and Postelthwaite (2005).

For the radiant system, we control the water flow rate using either a valve or variable speed pump, and close a feedback loop on the ceiling surface temperature. This is a simple proportional - integral (PI) design, with a closed-loop bandwidth tuned to be $\omega_{\mathrm{B}} = 0.001$ rad/s, giving a time constant of approximately 15 min. The DOAS system has two feedback loops. The evaporator superheat is measured and fed back through a PI compensator to actuate one of the electronic expansion valves (EEV). The building relative humidity is measured and fed back through a PI compensator to actuate the DOAS compressor frequency. These designs satisfy requirements 2-5, and allow for a building management system to provide separate temperature and humidity setpoints for improved human comfort and energy efficiency.

The design for the VRF is more subtle. It is tempting to close a feedback loop for the VRF compressor frequency (CF) on the room temperature tracking error(s). However, the transfer function from CF to the room temperatures is non-minimum phase, as demonstrated in the previous section, with a zero located at $z = 0.0015$. This will limit the achievable bandwidth of the controller to $\omega_B < z/2$ (see Skogestad and Postelthwaite (2005)), corresponding to a time constant of 8000 s, or 2 h, which does not meet our requirements and is generally bad practice. If we were to close a feedback loop on the room temperatures and increase the feedback gain to achieve a faster response, the closed-loop system will be unstable if an EEV saturates, which happens frequently.

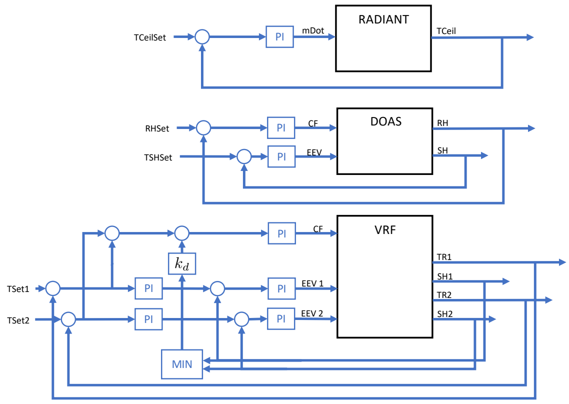

Figure 9: Feedback control architecture.

We instead adopt the cascade configuration shown in Figure 9. An inner loop for each EEV is closed on the evaporator superheat measurements for each indoor unit, using a PI compensator. An outer loop is then closed on each room temperature. This design allows for each zone to achieve a distinct temperature setpoint, and also enforces constraints on each EEV using a limiter and anti-windup. The feedback loop for the compressor frequency is then closed on an signal defined to be the sum of the room temperature errors *plus* the minimum evaporator superheat, weighted by a gain k_d. The transfer function from CF to this signal is non-minimum phase, but the offending zeros are far into the right-half plane, so that the feedback gain can be made sufficiently large to ensure a closed-loop bandwidth on room temperature to be $\omega_{\mathrm{B}} = 0.001$ rad/s, to match the transient response of the radiant system. Furthermore, the minimum superheat will be driven to a desired set-point, while the other superheats will assume whatever value is needed to achieve different zone temperature set-points. The overall design meets all of our requirements.

The closed-loop response of the linear system to a set-point change is shown in Figure 10 for constant conditions of 35 °C ambient temperature and 16 W/m^2 sensible and 4 W/m^2 latent heat gains. The top response is due to a -1 °C setpoint change in zone 1 air temperature. All other set-points are held constant. While the zone air temperature changes within 15 min, as designed, the mean radiant temperature (TRad) changes only -0.2 °C, and on a slower time constant, because it represents the mean temperature of the zone constructions, and these are cooled by the air, which has a slow response. Human comfort is a function of both air temperature and mean radiant temperature, equally, in office conditions (ASHRAE, 2017).

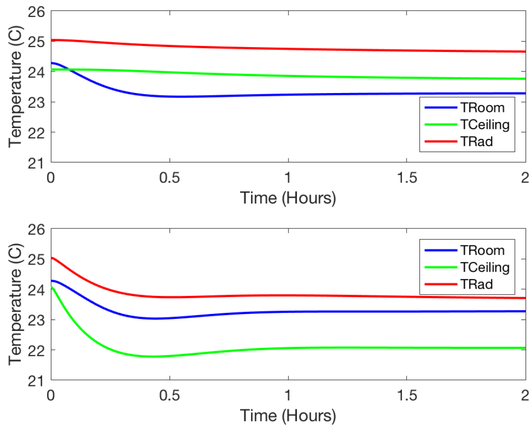

Figure 10: Temperature response of the integrated system, showing zone air temperature (TRoom), ceiling panel temperature (TCeiling), and zone mean radiant temperature (TRad), for a -1 ˚C setpoint change in air temperature (top), and a simultaneous -2 ˚C setpoint change in ceiling temperature (bottom).

Because of this slow radiant response, an average human would therefore experience only about 60% of the benefit of the set-point change. In the lower plot, the ceiling set-point is changed by -2 ˚C simultaneous with the -1 ˚C setpoint change in air temperature. Both respond with the same time constant by design. As a result, the mean radiant temperature changes by about -1 ˚C within 15 min, so the average human would experience the full -1 ˚C of setpoint change, which is what is probably desired. This improved thermal comfort does not come at a high energy cost; the total power consumption for the DOAS and multi-split system is about 82 W lower with the radiant ceiling control, while the radiant system (under the assumption of a constant thermal COP of 3) requires approximately 67 W of additional thermal load and 61 W of additional pumping power. This results in a net electrical power increase of only about 46 W.

Conclusions & Future Work

Current trends in high-performance buildings will impose new constraints and performance requirements on HVAC systems that may be best met with the use of multiple interacting subsystems. Such system architectures will have significantly improved performance if these multivariable dynamics can be shaped during the system design stage by the use of dynamic models of equipment and buildings. Future work includes the extension of the described process to size multiple interacting HVAC systems in consideration of both their steady-state performance and their dynamic behavior, as well as further improvements of the simulation speed that address the significant numerical stiffness of these systems.

References

ASHRAE (2017). *Thermal Environmental Conditions for Human Occupancy.*

Crawley, D., L. Lawrie, C. Pedersen, and F. Winkelmann (2000). EnergyPlus: energy simulation program. *ASHRAE Journal 42*, 49–56.

Gayeski, N., P. Armstrong, and L. Norford (2011). Predictive pre-cooling of thermo-active building systems with low-lift chillers. *HVAC&R Research 18*(5), 858–873.

Hong, T., K. Sun, R. Zhang, R. Hinokuma, S. Kasahara, and Y. Yura (2016). Development and validation of a new variable refrigerant flow system model in EnergyPlus. *Energy and Buildings 117*, 399–411.

Jeong, J.-W., S. Mumma, and W. Bahnfleth (2003). Energy conservation benefits of a dedicated outdoor air system with parallel sensible cooling by ceiling radiant panels. In *ASHRAE Transactions*, Volume 109, pp. 627–636.

Laughman, C., S. Bortoff, and H. Qiao (2018). Integrated control of multi-zone buildings with ventilation and VRF systems in cooling mode. In *Purdue High-Performance Buildings Conference.*

Laughman, C. and H. Qiao (2018). On closure relations for dynamic vapor compression cycle models. In *Proc. of the 1st American Modelica Conference*, Cambridge, MA, USA, pp. 67–76.

Modelica Association (2017). Modelica specification, Version 3.4.

Nouidui, T., K. Phalak, W. Zuo, and M. Wetter (2012). Validation and application of the room model of the Modelica Buildings library. In *Proc. of the 9th Int'l Modelica Conf.*, pp. 727–736.

Qiao, H., V. Aute, and R. Radermacher (2015). Transient modeling of a flash tank vapor injection heat pump system - Part I: Model development. *Int. J. Refrigeration 49*, 169–182.

Qiao, H., C. Laughman, D. Burns, and S. Bortoff (2017). Dynamic characteristics of an R410A multi-split variable refrigerant flow air-conditioning system. In *12th IEA Heat Pump Conference.*

Skogestad, S. and I. Postelthwaite (2005). *Multivariable Feedback Control: Analysis and Design.* Wiley.

U.S. Department of Energy (2015). *Methodology for estimating the cost-effectiveness of residential energy code changes.*

Wetter, M., W. Zuo, T. Nouidui, and X. Pang (2014). Modelica buildings library. *Journal of Building Performance Simulation 7*(4), 253–270.